Jurnal Teknologi

Full Paper

THE EXTERNAL DRAFT TUBE GASLIFT BIOREACTOR: HYDRODYNAMIC CHARACTERISTICS AND PARAMETRIC OPTIMIZATION

Mahmood K. H. Al-Mashhadani, Atheer M. Al-Yaqoobi, Rasha H. Salman*

Department of Chemical Engineering, College of Engineering, University of Baghdad, Baghdad, Iraq

Article history
Received
10 April 2024
Received in revised form
19 June 2024
Accepted
14 July 2024
Published Online
22 December 2024

*Corresponding author
rasha.habeeb@coeng.uobaghdad.edu.iq

Graphical abstract

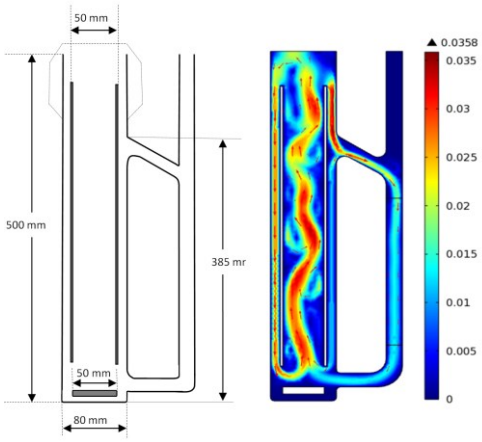

Abstract

Gaslift reactors are employed in several bioapplications due to their characteristics of cost-effectiveness and high efficiency. However, the nutrient and thermal gradient is one of the obstacles that stand in the way of its widespread use in biological applications. The diagnosis, analysis, and tracking of fluid paths in external draft tube gaslift bioreactor-type are the main topics of the current study. Several parameters were considered to assess the mixing efficiency such as downcomer-to-rizer diameter ratio (Ded/Dr), the position of the diffuser to the height of bioreactor ratio (Pd/Lr), and gas bubble size (Db). The multiple regression of liquid velocity indicates the optimal setting: Ded/Dr is (0.5), Pd/Lr is (0.02), and Db is (400) um. However, for technical and operational reasons, it was necessary to make some changes in the optimal values obtained from the numerical equations. The study also revealed that the size of gas bubbles is the characteristic that has the greatest influence on the dynamic efficiency of the fluid inside the bioreactor, since, reducing the bubble size by half can enhance the improvement rate in the circulation of the liquid up to 35%.

Keywords: Hydrodynamic, Gaslift, Optimization, Bioreactor, bubble size

1.0 INTRODUCTION

Gas-lift reactors (ALRs) have several advantages over conventional gas-liquid reactors such as bubble columns. Operational flexibility and scalability are important characteristics for many industrial applications [1, 2]. Therefore, this type of reactor is becoming more prevalent in biological wastewater treatment plants, chemical processes, and biochemical technologies [3, 4, 5, 6]. Up to now, and through several studies, bioreactor design optimization approaches have been followed to optimize the bioprocess's performance and reduce maintenance and operating costs [7– 10]. Despite significant scientific achievements in the design of gaslift reactors, it is commonly acknowledged that the design and scale-up of this reactor remain challenging due to the sophisticated multiphase flow regime [11, 12].

Internal and external circulation loop draft tubes are two main types of gaslift photo/bioreactors [1, 13, 14]. In the literature, many extensive theoretical and simulation studies have focused on estimating these hydrodynamic characteristics in internal loop reactors [15]. While the external loop gaslift bioreactor is also has a good residence time of

cultivation media in the riser region and external downcomer, in addition, controlled gas-phase disengagement at the top of the bioreactor are advantages of this type of bioreactor [16]. Moreover, for controlling the liquid velocity in both the riser and the downcomer of this type of bioreactor, the two zones (riser and downcomer zone) can be connected by a straightforward valve independently of the gas flux input rate. It is worthwhile to point out that the necessary portion of this reactor's heat exchange and temperature control systems can be controlled with high efficiency. In addition, accurate estimates of phase and velocity impedances in the up and down phase are necessary to construct an gaslift reactor with an external circulation loop. The aforementioned characteristics have made this kind of an appealing and promising option for several industrial applications [16– 20].

The current research aims to highlight on this type of reactor by tracking the paths of flow and circulation of liquid and gas inside the reactor according to the parametric analysis to assess the effects of geometrical and operational factors on mixing efficiency under situations related to microbubbl technology.

2.0 MATERIAL AND METHODS

2.1 Methodology of Taguchi Optimization Methodologies

It was necessary to use an effective numerical approach to identify the factors that have the greatest impact on the performance of the observed process and to exclude those that have less of an impact to comprehend how different parameters might alter a process's outcomes or regulate its efficiency. In this study, the Taguchi optimization methodologies as the design of modeling in Minitab software was employed to investigate the effect of various geometry variables (Bubble diameter (Db, m), diameter of external downcomer tube to diameter of bioreactor (Ded/Dr), position of bubbling diffuser according to height of bioreactor (Pd/Lr)) on the response of liquid velocity profiles in external loop gaslift reactor. Four levels of these variables were adopted in this modelling to get 16 run (L16_orthogonal arrays), while the velocity of circulation liquid in the bioreactor was taken as desired response as shown in Tables 1. In this optimization approach, while the outside and inner orthogonal arrays have been taken into consideration to lessen the noise effects in physical testing, multiple experiments were carried out at the array's center point to estimate the mean and standard deviation.

The primary objective of the current investigation is to maximize the liquid velocity profile value; therefore, the higher is best of S/N ratio analysis was used [21, 22]. The S/N ratio was calculated according to Equation (1) [23].

$$\frac{S}{N} = -\log\left[\frac{1}{n}\sum_{i=1}^{n}\frac{1}{y_i^2}\right] \quad (1)$$

Table 1 Geometry variables of external loop gaslift bioreactor

Parameters	Symbol	Units	Levels			
			1	2	3	4
Bubble Diameter	Db	m	0.0004	0.0007	0.001	0.003
diameter of external downcomer tube/ Diameter of bioreactor	Ded/Dr	-	0.125	0.25	0.375	0.5
Position of bubbling diffuser/Height of bioreactor	Pd/Lr	-	0.02	0.06	0.1	0.14

Where, n and y represent the number of observations and the perceived response.

2.2 The Mathematical Model

In this study, the hydrodynamic characterization in the external loop gaslift bioreactor was evaluated through the circulation liquid velocity. Two-dimension geometry was adopted in the computational domain. Figure 1 shows the configuration of the simulated bioreactor used in the current investigation. In recent years, COMSOL Multiphysics, as computational software, has become widely employed in the design of chemical reactors, due to advancements in computer hardware and software, as well as advances in numerical algorithms and fluid dynamics theories. The current study's equations were based on the time-dependent conservation of momentum of the fluid inside the bioreactor. The computational fluid model's everlasting loop gas-lift bioreactor schematic is shown in Figure 1.

The laminar flow model with transport dilute species interface was adopted to model the mixture of gas-liquid regimes in an external loop circulation gaslift reactor according to the following dynamic transport Equations.

$$\varnothing_L \rho_L \frac{\partial u_L}{\partial t} + \varnothing_L \rho_L (u_L.\nabla)u_L = \nabla.\left[-\mathrm{pI} + \varnothing_L \eta_L \left(\nabla u_L + (\nabla u_L)^{\mathrm{T}}\right)\right] + \varnothing_L \rho_L g + F \quad (2)$$

$$\frac{3\mathrm{Cd}}{4\mathrm{d_b}} \rho_L \left|u_{slip}\right| u_{slip} = -\nabla P \quad (3)$$

$$\mathrm{Cd} = \frac{16}{Re_b} \quad (4)$$

$$Re_b = \frac{\mathrm{d_b}\rho_L \left|u_{slip}\right|}{\eta_L} \quad (5)$$

Where $\varnothing_L$ is liquid volume fraction, ρ_L is density of liquid kg/m^3, u_L is Velocity of liquid phase m/s, t is time (s), η_L is dynamic viscosity of liquid Pa.s, g is gravity

m/s^2, F is volume force N/m^3, d_b is bubble diameter (m), Cd is viscous drag coefficient, Re_b is Reynolds number, and u_{slip} is relative velocity (m/s).

The liquid boundaries condition in all walls of the reactor was set to no-slip conditions (i.e: u_L,-$n.N_{\rho g \phi g}$, -$n.N_n$ were set to zero) except for the bubble flow diffuser position and the top reactor's two outlets.

In top surface of the bubbling diffuser, the gas mass flux was 0.009 kg/(m^3.s), while the boundary condition of the liquid was no slip. Thus, -$n.N_{\rho g \phi g}$ = $N_{\rho g \phi g}$ and the number density were calculated according to:

$$-n.N_n = N_n \tag{6}$$

The slip condition was adopted as the liquid boundary condition on the surface of the liquid of the reactor, while the gas boundary condition was determined as the gas outlet option.

$$-u_L.n = 0 \tag{7}$$

$$K-(K.n)n = 0 \tag{8}$$

$$K = \left[\mu_L\left(\nabla u_L + (\nabla u_L)^T\right)\right]n \tag{9}$$

In the current work, convection-driven transport of diluted species was simulated using the transport of diluted species interface in two dimensions model where the time depended was studied:

$$\frac{dci}{dt} + \nabla.\left(D_i \nabla c_i\right) + u.\nabla c_i = R_i \tag{10}$$

$$N_i = -D_i \nabla c_i + uc_i \tag{11}$$

Where c_i is Concentration of species i, D_i is diffusion coefficient for species i, and R_i is rate of reaction for species i. The maximum element growth rate was 1.15 with the resolution of curvature being 0.3.

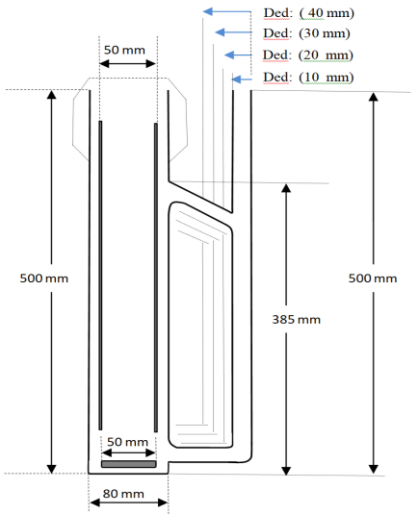

Figure 1 Schematic of the eternal loop gas-lift bioreactor used in the computational fluid model: The square dotes represent the dimensions of external loop draft tube that were dealt with in the study

3.0 RESULTS AND DISCUSSION

The existence of environmental and nutritional imbalances may cause bacteria to stop growing biologically, decreasing the overall productivity of the bioreactor. Several operating conditions can create these undesirable gradients in biological processes. Providing appropriate and homogeneous conditions with adequate provision for process requirements is the responsibility of mixing in the bioreactor. The velocity non-distribution profiles of the fluid inside the bioreactor are one of the reasons for generating the thermal and nutrient gradient. As a result, the current study assessed the performance of the bioreactor by measuring fluid velocity inside the bio-system. Therefore, the effect of three geometric parameters (bubble diameter, external downcomer tube, and position of the diffuser) on the bioreactor performance was verified. The evaluation indicator was the average fluid velocity in the riser and downcomer area. The Taguchi optimization method was adopted in this evaluation study. The goal was not to reduce the number of experiments only but rather to study the interaction between these influences and determine which parameters have the most influence on the performance of the bioreactor. Table 2 displays the liquid velocity response in the external loop gaslift bioreactor using the Taguchi optimization approach according to changes in the value of suggested parameters.

Table 2 Response of liquid velocity used in Taguchi optimization of external loop gaslift bioreactor according to Geometry variables

Db	Ded/Dr	Pd/Lr	Response
0.0004	0.125	0.02	0.0049
0.0004	0.25	0.06	0.0057
0.0004	0.375	0.1	0.0063
0.0004	0.5	0.14	0.0051
0.0007	0.125	0.06	0.0023
0.0007	0.25	0.02	0.0029
0.0007	0.375	0.14	0.0029
0.0007	0.5	0.1	0.0036
0.001	0.125	0.1	0.0014
0.001	0.25	0.14	0.0015
0.001	0.375	0.02	0.0021
0.001	0.5	0.06	0.0024
0.0013	0.125	0.14	0.000973
0.0013	0.25	0.1	0.0011
0.0013	0.375	0.06	0.0014
0.0013	0.5	0.02	0.0017

Figure 2 is the means of signal noise ratio against the level of factors: (bubble diameter (Dd), diameter of downcomer to diameter of rizer, (Ded/Dr), position of the diffuser to height of bioreactor (Pd/Lr)). The results demonstrate how each factor under study has an impact on the fluid velocity response of the bioreactor. It also shows that, in comparison to the diameter of the return tube (external downcomer tube) and the placement of the diffuser, the diameter of the bubbles has more of an effect on the

liquid velocity. In addition that the diffuser's placement doesn't have as much of an impact on the response as other factors, therefore moving it won't have the same impact on mixing efficiency. The multiple regression of liquid velocity indicates the optimal setting is Db is 400 um, Ded/Dr is 0.5, and Pd/Lr is 0.02.

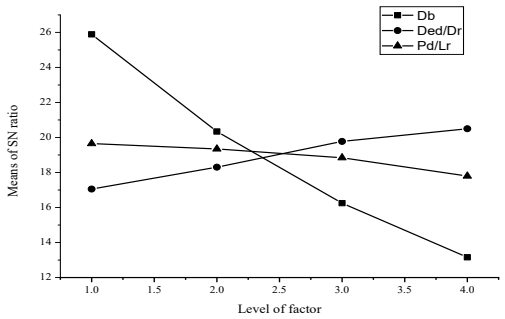

Figure 2 Liquid velocity graph for means signal to noise ratio

The utilization of analysis of variance (ANOVA) by Taguchi method is an excellent tool to detect the most statically significant parameter and to conquer the value of the percentage contribution of each studied factor. This statistical analysis provides an opportunity to understand the interaction and contribution of parameters and their importance on the bioreactor's mixing efficiency [24, 25]. ANOVA analysis was addressed as a methodology for optimizing the outcomes of the present study and the results are illustrated in Table 3. Statistically, F test is a tool utilized to perceive which design factors have a significant influence on the quality characteristic. In other words, the F-ratio is traditionally used to conclude the importance of a parameter [26]. This importance can be concluded from high values of F ratio either when it is > 4 which indicates that any small change in this parameter would give a significant effect on the quality characteristic [27]. The data obtained from the ANOVA table show that the size of the bubbles has the greatest effect on the response of the circulation liquid velocity in the bioreactor if it is compared with the diameter of the external downcomer tube and the location of the diffuser. This was evident from the high contribution percentage of bubble diameter as well as the high value of F-value and very low P-value. Also, based on ANOVA results, the diameter of the external downcomer tube has the highest effect, while the effect of the diffuser location was the lower one.

Table 3 Analysis of variance (ANOVA) for circulation liquid velocity measurement

Source	DF	Seq SS	Contribution%	Adj SS	Adj MS	F-Value	P-Value
Db	3	0.000042	93.19	0.000042	0.000014	99.63	0
Ded/Dr	3	0.000002	3.86	0.000002	0.000001	4.12	0.066
Pd/Lr	3	0	1.09	0	0	1.16	0.399
Error	6	0.000001	1.87	0.000001	0		
Total	15	0.000045	100.00				

Figure 3 shows the profile of liquid velocity magnitude at optimized values, Db (400 um), Ded/Dr (0.5), and Pd/Lr (0.02) at different periods. Increasing the cross-section area of the external loop pipe offers adequate space for the fluid in this region of the bioreactor and allows it to travel freely. The liquid velocities in the downcomer and riser regions are dictated by frictional losses, which are determined by the shape of the gaslift bioreactor and operating conditions. This cross-section, on the other hand, creates disruptions followed by rotating motions, leaving comparatively lifeless zones behind. Therefore, by tracing the paths of the fluid in the return tube, Figure 3 indicates the generation of relatively dead areas in a specific place in the downcomer tube. Perhaps the widening of the cross-section of the return pipe allowed the fluid to pass certain paths but not others, causing the generation of regions of gradual velocity, which may later result in a gradient in temperature and nutrient concentration and put the microorganisms in a state of famine. As a result, the current study advocated lowering the bioreactor's cross-section to address these challenges in various spots inside the bioreactor as shown in Figure 4.

In another aspect, the nature of some chemical and biological environments can contribute to the accumulation of solids of different sizes on the surface of the diffuser at the bottom of the bioreactor, making it difficult to maintain the bioreactor and causing clogging of the micropores of the diffuser as well as causing a useful volume of the bioreactor to be out of service. Therefore, the present study proposes a certain location of the diffuser (Pd/Lr (0.04)) to facilitate the maintenance of the bioreactor and the diffuser, remove solids from the bottom of the bioreactor, and reduce the dead zone in the bottom part of the bioreactor as shown in Figure 4,B.

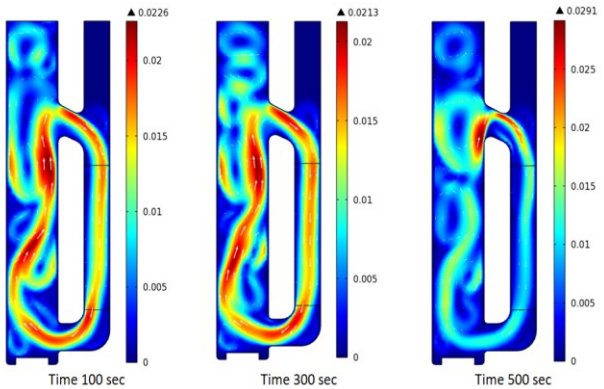

Figure 3 Profile of liquid velocity magnitude at optimized values, Db (400 um), Ded/Dr (0.5), Pd/Lr (0.02) at different period time

Figure 5 displays the horizontal profile of liquid velocity, y component, at a height of 25 cm from the base of the bioreactor (scale from the bottom of

bioreactor) with optimized values (Db (400 um), Ded/Dr (0. 5), and Pd/Lr (0.02)) and suggested values (Db (400 um), Ded/Dr (0.25), and Pd/Lr (0.04)).

The modeling data reveals dispersion and turbulence in downcomer fluid routes at the values (Db (400 um), Ded/Dr (0. 5), and Pd/Lr (0.02)), compared to stability in the paths in the same region if the (Db (400 um), Ded/Dr (0.25), and Pd/Lr (0.04) were adopted. This stability adds to the regularity of mixing inside the bioreactor as well as the microbes' consistent access to food and acceptable ecosystems.

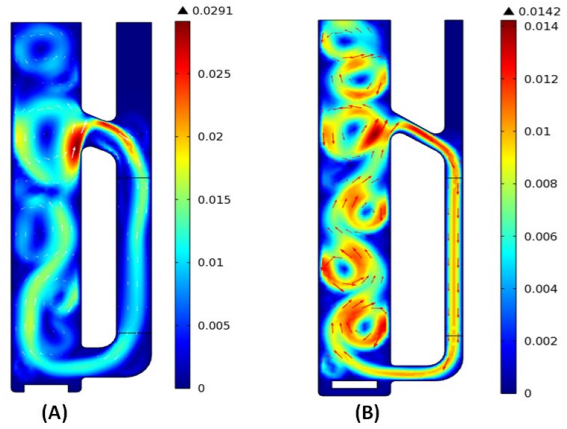

Figure 4 Profile of liquid velocity magnitude (A) optimized values, Db (400 um), Ded/Dr (0. 5), Pd/Lr (0.02) (B) suggested values, Db (400 um), Ded/Dr (0.25), Pd/Lr (0.04)

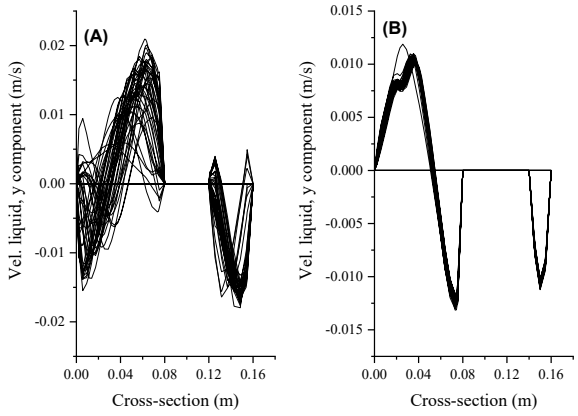

Figure 5 Horizontal profile of liquid velocity, in y component, at a height of 25 cm from the base of the bioreactor (A) optimized values, Db (400 um), Ded/Dr (0. 5), Pd/Lr (0.02) (B) suggested values, Db (400 um), Ded/Dr (0.25), Pd/Lr (0.04)

Typically, the turbulent eddies generation depends on the bioreactor size and Reynolds number. Different scales of turbulences coexist and are superimposed to mean flow. These turbulences increase in size as the fluid velocity increases inside the bioreactor. Inside larger turbulence eddies, smaller turbulence eddies usually exist. These eddies can potentially result in low yield and quality of the final product, when producing cell and gene treatments, for example, weaker cells may have their integrity compromised by shear created by turbulent flow [28].

In the present model, and under the operational conditions used, the central velocity in the riser region also contributed to the generation of turbulent vortices in the fluid paths, which may somewhat resemble a bubble column bioreactor. Therefore, the draft tube may be the key to solving these vortexes. The stability of the tracks of the fluid in the rizer area was observed when installing this inner tube in this area, as shown in Figure 6. In addition, it can be observed that multiple paths have been formed with good flow inside the bioreactor (One rizer, and two downcomer regions). Where the fluid passes into the riser area, it will go either to the internal downcomer area or to the external downcomer area with a smooth and stable path. This may significantly reduce the feed and operational gradients in the bioreactor. In photobioreactors, for example, the living organisms that need light as an essential element in self-photosynthesis, this design will ensure that the largest number of living cells receive a sufficient amount of light source.

The agitation resulting from rising air bubbles inside the bioreactor represents a driving force towards strengthening the turbulence of the liquid, enhancing transfer phenomena and providing sufficient contact time for gas bubbles and biomedium. As a result, the current study emphasized the surface area covered by microbubbles, while keeping their size constant on the fluid paths and agitation efficiency.

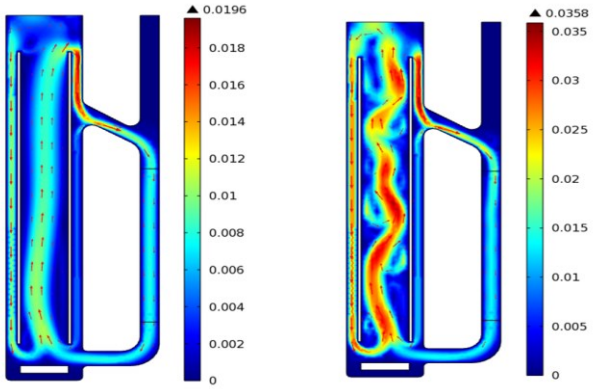

Figure 6 Profile of liquid velocity magnitude under suggested values, Db (400 um), Ded/Dr (0.25), Pd/Lr (0.04) (A) with internal-external draft tube at 400 um bubble diameter, (B) with internal draft tube at 200 um bubble diameter

Figure 7 displays the horizontal profile of liquid velocity, in y component, at a height of 25 cm from the base of the bioreactor at optimized values (Db (400 um), Ded/Dr (0.25), and Pd/Lr (0.04)) and suggested values (Db (200 um), Ded/Dr (0.25), Pd/Lr (0.04)). The modeling data show consistency and organization in the paths of the fluid with microbubbles diameter of (400 microns) and with

smaller ones with a diameter of 200 microns, which reflects the effect of the inner tube on organizing the paths according to high coordination, as well as increasing the mixing efficiency. The force generated at the riser area results from the rising microbubbles, and although most of its strength is lost at the top of the bioreactor, it causes three paths to be generated in opposite directions. It ensures a homogeneous distribution of the liquid over all parts of the bioreactor as well as improved transfer processes. However, there may be limitations in the positive effect of microbubble diameter on mixing efficiency in the bioreactor. The findings of the study by Al-Mashhadani *et al*. (2015) [14] showed that when the bubble diameter is lowered to less than 100 microns, the fluid velocity drops regardless of the kind of bioreactor employed. However, a well-selected diffuser material that offers superior wettability can provide a significant reduction in bubble size. Additionally, the characteristics of the liquid medium are crucial in determining the size of the bubble that is formed [29].

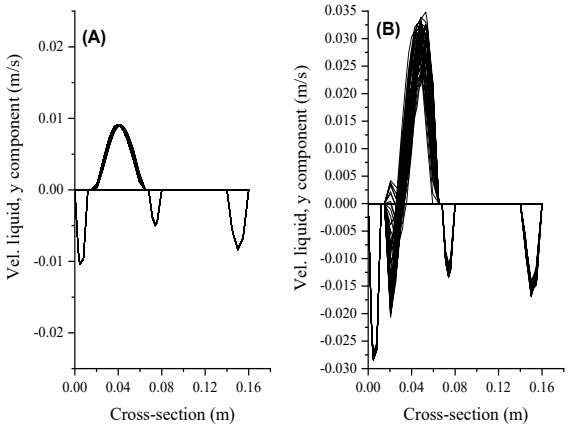

Figure 7 Horizontal profile of liquid velocity, y component, at a height of 25 cm from the base of the bioreactor with suggested values, Db (400 um), Ded/Dr (0.25), Pd/Lr (0.04) (A) with internal draft tube at 400 um bubble diameter, (B) with internal draft tube at 200 um bubble diameter

The current investigation has also explained this situation through the concentration of gas bubbles in the lower section of the bioreactor preventing the recirculation of liquid around the internal draft tube due to the buoyant force of the bubbles being greater than the force pushing the liquid downward in the bioreactor. Therefore, the diameter of the gas bubbles used in the bioreactor may target a specific type of application [30, 31].

Through efficiency monitoring, the most crucial fundamental components influencing bioreactor design were the focus of the current study. Nonetheless, the gas flow rate may also have an impact on the bioreactor's liquid distribution velocity. The impact of momentum imparted to the liquid and its intimate relationship to the gas rate fed to the bioreactor were covered by [16]. In addition to lowering the momentum transmitted to the biological fluid, increasing the gas velocity also modifies the size of the gas bubbles, which will have an adverse effect on the transfer phenomena (mass and heat transfer). The current study thus made an effort to steady the flow rate to avoid interfering with other variables, particularly the bubble width.

The tracer injection was also addressed in the current study as an approach for evaluating dye delivery and analyzing the residence time distribution in tubular bioreactors. The dynamic study of this type of bioreactor dealt with the concentration of the substance that is injected from the diffuser area. The speed of sensing the concentrated material in the fluid was another measure of the mixing performance in the bioreactor. Figure 8 shows that the speed of sensitization of the concentrated substance in the fluid under the optimization conditions was faster than the optimal conditions. For example, at a certain area of the bioreactor, reducing the diameter of the gas bubble from 400 microns to 75 um improves the mixing efficiency to 35 %.

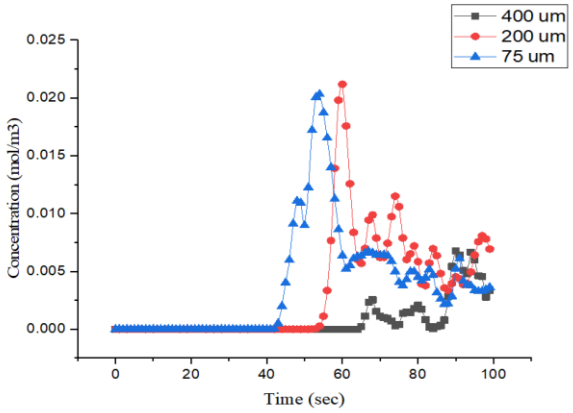

Figure 8 Tracer injection concentration of the liquid (A) optimized values, Db (200 um), Ded/Dr (0.5), Pd/Lr (0.02) (B) suggested values, Db (200 um), Ded/Dr (0.25), Pd/Lr (0.04) and Db (75 um), Ded/Dr (0.25), Pd/Lr (0.04)

Figure 9 displays the influence of the external return pipe cross-section on fluid velocity for all cases considered. Under the operational and design conditions deduced from the equations of numerical methods, the fluid velocity profile appears to have irregular paths. The response shows a noticeable variation in the maximum fluid velocity at the same cross-section and for the same design and operating conditions as previously mentioned. The results also demonstrated that sticking to particular pathways through the decreasing cross-section enhances the homogeneity of the fluid velocity inside the outer tube. It also appears that the suggested internal draft tube in the area of the riser to be inserted to improve the paths in that area did not affect the regularity of the paths in the external tube, except for a decrease

in the central velocity of the fluid. This is due to the reduced driving force as a result of its distribution between the internal and external downcomer as illustrated in Figure 6.

However, the effective variable in the story of mixing efficiency in the bioreactors (meaning the diameter of the air bubbles) has a role in modifying this situation, since lowering the diameter of the bubbles enhances the central velocity of the fluid in the external downcomer zone.

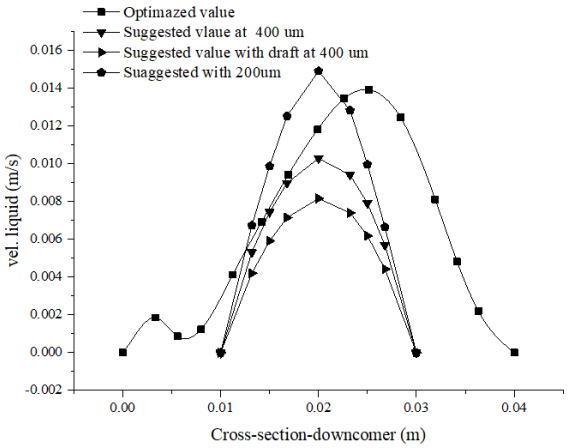

Figure 9 Liquid velocity in the downcomer region at optimized value (Db (200 um), Ded/Dr (0.5), Pd/Lr (0.02)), Suggested value (Db (400 um), Ded/Dr (0.25), Pd/Lr (0.04)) , Suggested value at with draft tube at (Db (400 um), Ded/Dr (0.25), Pd/Lr (0.04), Suggested value at with draft tube at Db (200 um), Ded/Dr (0.25), Pd/Lr (0.04)

4.0 CONCLUSION

The current research investigated the fluid dynamics inside the bioreactor under different operational and structural conditions. Takeuchi's method was used to determine the optimum boundary conditions and structural conditions that have an impact on the mixing performance of the bioreactor. This method was integrated with COMSOL Multiphysics simulation through mathematical equations for fluid transfer within the bioreactor as a valuable tool for examining and analyzing fluid tracking, residence time distribution, and mixing efficiency. The current comprehensive method aided in the study of fluid tracking within the bioreactor, offering thorough process knowledge of basic transport processes. The tracer injection process as an analysis approach has shown the improvement of mixing efficiency by 35% with 75 um bubble diameter compared with 400 um bubble diameter in the same operating conditions.

Acknowledgement

The authors would like to express their gratitude to the University of Baghdad and the Iraqi Ministry of Higher Education and Scientific Research. They also express gratitude to the Department of Chemical Engineering-College of Engineering and the Department of Biology-College of Science for their assistance. Furthermore, they would want to convey their heartfelt appreciation to the University of Sheffield in the United Kingdom.

Conflicts of Interest

The author(s) declare(s) that there is no conflict of interest regarding the publication of this paper.

References

[1] Naidoo, N., Pauck, W. J. & Carsky, M. 2021. Effects of Sparger Design on the Gas Holdup and Mass Transfer in a Pilot Scale External Loop Airlift Reactor. *South African Journal of Chemical Engineering*. 37(May): 127–134. Doi: https://doi.org/10.1016/j.sajce.2021.05.009.

[2] Ibrahim, A. R. & Abdulmajeed, B. A. 2018. Biological Co-existence of the Microalgae – Bacteria System in Dairy Wastewater using Photo-bioreactor. *Iraqi Journal of Chemical and Petroleum Engineering*. 19(3): 1–9. Doi: https://doi.org/10.31699/IJCPE.2018.3.1.

[3] Xing, C., Wen, J., Li, W., Shi, J., Wang G. & Xie, J. 2023. Integrating the Fe^{2+}/H_2O_2-strengite Method in Airlift Reactor for Phosphorus Removal and Recovery from Organic Phosphorus Wastewater. *Chemical Engineering Journal*. 475: 146093. Doi: https://doi.org/10.1016/j.cej.2023.146093.

[4] Ammar, S. H., Ismail, N. N., Ali, A. D. & Abbas, W. M. 2019. Electrocoagulation Technique for Refinery Wastewater Treatment in an Internal Loop Split-Plate Airlift Reactor. *Biochemical Pharmacology*. 7(6): 103489. Doi: https://doi.org/10.1016/j.jece.2019.103489.

[5] Mahata, C., Mishra, S., Dhar, S., Ray, S., Mohanty, K. & Das, D. 2023. Utilization of Dark Fermentation Effluent for Algal Cultivation in a Modified Airlift Photobioreactor For Biomass and Biocrude Production. *Journal of Environmental Management*. 330: 117121. Doi:https://www.sciencedirect.com/science/article/pii/S0301479722026949.

[6] Ibrahim, A. R. & Abdulmajeed, B. A. 2018. Mass Transfer Study for Bio-Synergy in Dairy Wastewater Treatment Plant. *Journal of Engineering*. 24(9): 51–63. Doi: https://doi.org/10.31026/j.eng.2018.09.04.

[7] Moradi, S., Zinatizadeh, A. A., Zinadini, S. & Gholami, F. 2021. High-rate CNP Removal from Wastewater in A Single Jet Loop Air Lift Bioreactor : Process Modeling and Optimization with Four Process and Operating Factors. *Journal of Water Process Engineering*. 40: 101980. Doi: https://doi.org/10.1016/j.jwpe.2021.101980.

[8] Mulakhudair, A. R., Al-Mashhadani, M. K. H. & Kokoo, R. 2022. Tracking of Dissolved Oxygen Distribution and Consumption Pattern in a Bespoke Bacterial Growth System. *Chemical Engineering & Technology*. 45(9): 1683–1690. Doi: https://doi.org/10.1002/ceat.202200209.

[9] Al-Mashhadani, M. K. H. 2017. Heat Transfer and Hydrodynamic in Internal Jacket Airlift Bioreactor with Microbubble Technology. *Iraqi Journal of Chemical and Petroleum Engineering*. 18(4): 35–45. Dol: https://doi.org/10.31699/IJCPE.2017.4.4.

[10] Jose, J., Kallupurakel, T.J., Shibin S P & Manirethan, V. 2024. Optimizing Chlorella Vulgaris Cultivation in an Airlift Photobioreactor using Coconut Oil Mill Effluent (COME) for

Biodiesel Production. *Journal of the Indian Chemical Society*. 101(3): 101132.
Doi: https://doi.org/10.1016/j.jics.2024.101132.

[11] Yang, C. & Mao, Z.-S. 2014. Chapter 4 - Airlift Loop Reactors. In: Yang, C. & Mao, Z.-S (eds.). Numerical Simulation of Multiphase Reactors with Continuous Liquid Phase. Oxford: Academic Press.
Doi:https://www.sciencedirect.com/science/article/pii/B9780080999197000044.

[12] Álvarez, C., Colón, J., Lópes, A. C., Fernández-Polanco, M., Benbelkacem, H. & Buffièr, P. 2018. Hydrodynamics of High Solids Anaerobic Reactor : Characterization of Solid Segregation and Liquid Mixing Pattern in a Pilot Plant VALORGA Facility under Different Reactor Geometry. *Waste Management Journal.* 76(June): 306–314.
Doi: https://doi.org/10.1016/j.wasman.2018.02.053.

[13] Wen, X., Liang, D., Hu, Y., Zhu, X., Wang, G. & Xie, J. 2023. Performance and Mechanism of Simultaneous Nitrification and Denitrification in Zeolite Spheres Internal Loop Airlift Reactor. *Bioresource Technology*. 380: 129073.
Doi: https://doi.org/10.1016/j.biortech.2023.129073.

[14] Al-Mashhadani, M. K. H., Wilkinson, S. J. & Zimmerman, W. B. 2015. Airlift Bioreactor for Biological Applications with Microbubble Mediated Transport Processes. *Chemical Engineering Science*. 137: 243–253.
Doi: https://doi.org/10.1016/j.ces.2015.06.032.

[15] Lestinsky, P. Vayrynen, Vecer, M., Wichterle, K. 2012. Hydrodynamics of Airlift Reactor with Internal Circulation Loop: Experiment vs. CFD Simulation. *Procedia Engineering.* 42: 974–991.
Doi: https://doi.org/10.1016/j.proeng.2012.07.482.

[16] Marroquín-Fandiño, J. E., Ramírez-Acosta, C. M., Luna-Wandurraga, H. J., Valderrama-Rincón, J. A., Cruz, J. C., Reyes, L. H. & Valderrama-Rincon, J. D. 2020. Novel External-loop-airlift Milliliter Scale Bioreactors for Cell Growth Studies: Low Cost Design, CFD Analysis and Experimental Characterization. *Journal of Biotechnology*. 324: 71–82.
Doi: https://doi.org/10.1016/j.jbiotec.2020.09.022.

[17] Mazziero, V. T., Batista, V. G., de Oliveira, D. G., Scontri, M., de Paula, A. V. & Cerri, M. O. 2022. Characterization of Packed-bed in the Downcomer of a Concentric Internal-loop Airlift Bioreactor. *Biochemical Engineering Journal.* 181: 108407.
Doi: https://doi.org/10.1016/j.bej.2022.108407.

[18] Hamood-ur-rehman, M., Dahman, Y. & Ein-mozaffari, F. 2012. Investigation of Mixing Characteristics in a Packed-bed External Loop Airlift Bioreactor Using Tomography Images. *Chemical Engineering Journal.* 213: 50–61.
Doi: https://doi.org/10.1016/j.cej.2012.09.106.

[19] Fontana, R.C. & da Silveira, M. M. 2012. Production of Polygalacturonases by Aspergillus Oryzae in Stirred Tank and Internal- and External-loop Airlift Reactors. *Bioresource Technology*. 123: 157–163.
Doi: https://doi.org/10.1016/j.biortech.2012.07.053.

[20] Teli, S. M. & Mathpati, C. S. 2020. Experimental and Numerical Study of Gas-Liquid Flow in a Sectionalized External-Loop Airlift Reactor. *Chinese Journal of Chemical Engineering.* 32: 39–60.
Doi: https://doi.org/10.1016/j.cjche.2020.10.023.

[21] Googerdchian, F. Moheb, A., Emadi, R. & Asgari, M. 2018. Optimization of Pb (II) Ions Adsorption on Nanohydroxyapatite Adsorbents by Applying Taguchi Method. *Journal of Hazardous Materials.* 349: 186–194.
Doi: https://doi.org/10.1016/j.jhazmat.2018.01.056.

[22] Madan, S. S. & Wasewar, K. L. 2017. Optimization for Benzeneacetic Acid Removal from Aqueous Solution using CaO_2 Nanoparticles based on Taguchi Method. *Journal of Applied Research and Technology*. 15(4): 332–339.
Doi: https://doi.org/10.1016/j.jart.2017.02.007.

[23] Ibrahim, H. M. & Salman, R. H. 2022. Study the Optimization of Petroleum Refinery Wastewater Treatment by Successive Electrocoagulation and Electro-oxidation Systems. 23(1): 31–41.
Doi: https://doi.org/10.31699/IJCPE.2022.1.5.

[24] Abbas, A. S., Hafiz, M. H. & Salman, R. H. 2016. Indirect Electrochemical Oxidation of Phenol Using Rotating Cylinder Reactor Indirect Electrochemical Oxidation of Phenol Using Rotating Cylinder Reactor. *Iraqi Journal of Chemical and Petroleum Engineering.* 17(4): 43–55.
Doi: https://doi.org/10.31699/IJCPE.2016.4.5.

[25] Mitra, A. S., Jawarkar, M., Soni, T. & Kiranchand, G. R. 2016. Implementation of Taguchi Method for Robust Suspension Design. *Procedia Engineering*. 144: 77–84.
Doi: https://doi.org/10.1016/j.proeng.2016.05.009.

[26] Barman, G., Kumar, A. & Khare, P. 2011. Removal of Congo Red by Carbonized Low-Cost Adsorbents: Process Parameter Optimization Using a Taguchi Experimental Design. *Journal of Chemical & Engineering Data*. 56(11): 4102–4108.
Doi: https://doi.org/ 10.1021/je200554z.

[27] Salman, R. H. 2019. Removal of Manganese Ions (Mn^{2+}) from a Simulated Wastewater by Electrocoagulation/ Electroflotation Technologies with Stainless Steel Mesh Electrodes: Process Optimization Based on Taguchi Approach. *Iraqi Journal of Chemical and Petroleum*, 20(1): 39–48.
Doi: https://doi.org/10.31699/IJCPE.2019.1.6.

[28] Iurashev, D., Jones, P.A., Andreev, N., Wang, Y., Iwata-Kajihara, T., Kraus, B. & Bort J. A. H. 2023. Scaling Strategy for Cell and Gene Therapy Bioreactors Based on Turbulent Parameters. *Biotechnology Journal.* 19: 2300235.
Doi: https://doi.org/10.1002/biot.202300235.

[29] Al-yaqoobi, A. M.G. & Zimmerman, W. B. 2023. Relative Wettability Measurement of Porous Diffuser and Its Impact on the Generated Bubble Size. *Chemical and Process Engineering.* 43(1): 45–55.
Doi: https://doi.org/10.24425/cpe.2022.140810.

[30] Al-yaqoobi, A., Hogg, A. D. & Zimmerman, W. B. 2016. Microbubble Distillation for Ethanol-Water Separation. *International Journal of Chemical Engineering*. 2016: 1–10.
Doi: https://doi.org/10.1155/2016/5210865.

[31] Tuan Van Le, Imai, T., Higuchi, T., Doi, R., Teeka, J., Xtaofeng, S. & Teerakun, M. 2012. Separation of oil-in-water Emulsions by Microbubble Treatment and the Effect of Adding Coagulant or Cationic Surfactant on Removal Efficiency. *Water Science & Technology.* 66(5): 1036–1043.
DOI: https://doi.org/10.2166/wst.2012.276.